What does a slug test measure: An investigation of instrument response and the effects of heterogeneity

Roger Beckie

Department of Earth and Ocean Sciences, University of British Columbia, Vancouver, British Columbia, Canada

Charles F. Harvey

Ralph M. Parsons Laboratory, Department of Civil and Environmental Engineering, Massachusetts Institute of Technology, Cambridge, Massachusetts, USA

Received 16 November 2001; revised 17 July 2002; accepted 17 July 2002; published 14 December 2002.

[1] We consider parameters determined by the inversion of slug-test head recovery data with the homogeneous-parameter model of *Cooper et al.* [1967] to be weighted spatial averages of transmissivity and storage defined at a smaller scale. We quantify the spatial averaging using a power-average spatial filter expression. We determine the form of the filter function and the power exponent using numerically simulated slug-test data. The filter function that describes how smaller-scale transmissivity is weighted by slug tests displays an approximate $1/r^2$ behavior, with r the radial distance from the well. The radius of the cylinderical volume that is averaged by the slug test is inversely proportional to the square root of the storage coefficient (larger averaging volume with smaller storage). The power exponent grows from -0.19 to 0.345 as the ratio of the characteristic scale of the heterogeneity to the characteristic scale of the averaging volume grows, although a power exponent of zero, corresponding to geometric averaging, provides good results for most simulations. Our results show that while slug tests are useful to estimate transmissivity, they have dubious value for estimating storage coefficients. We find that the transmissivity estimate is unbiased and does not appear to be strongly influenced by storage properties. The storage coefficient estimate is, however, strongly influenced by the transmissivity and is biased. We investigate the interaction between storage coefficient and transmissivity by examining an analytical slug-test model that contains two annular zones, each with distinct transmissivity and storage coefficient. *INDEX TERMS:* 1829 Hydrology: Groundwater hydrology; 1894 Hydrology: Instruments and techniques; *KEYWORDS:* slug test, groundwater, transmissivity, hydrology

Citation: Beckie, R., and C. F. Harvey, What does a slug test measure: An investigation of instrument response and the effects of heterogeneity, *Water Resour. Res.*, *38*(12), 1290, doi:10.1029/2001WR001072, 2002.

1. Introduction

[2] Slug tests are used to characterize the hydraulic conductivity and storage properties of the subsurface. While the natural subsurface is always heterogeneous to some degree, slug-test data are usually interpreted with simple analytic models that contain spatially homogeneous parameters. The objective of this work is to investigate how smaller-scale heterogeneities affect slug-test derived parameter values. We consider the homogeneous parameters identified with simple slug-test models to be spatial averages of heterogeneous parameters in the near-well region. In this paper we therefore investigate the type and scale of averaging that occurs when slug-test data are analyzed to determine hydraulic parameters.

[3] This work is motivated by the observation that the parameter values determined by slug-test analyses often differ from those determined at the same location using other testing methods, such as larger-scale pumping tests or smaller-scale core tests [*Butler and Healey*, 1998]. The difference in the results can in part be explained by the different volumes of the subsurface that are sampled, or averaged, by each test method. It is important to understand these support volume effects when interpreting hydraulic tests.

[4] Many researchers define the range or scale of a slug test, and thereby the volume investigated by the slug test, as that distance at which the head perturbation caused by the slug test has dissipated to a specified fraction of the initial excess head at the well bore [*Barker and Black*, 1983; *Guyonnet et al.*, 1993; *Karasaki et al.*, 1988; *Ramey et al.*, 1975; *Sageev*, 1986]. *Karasaki et al.* [1988] and *Guyonnet et al.* [1993] show that for two-dimensional flow conditions this perturbation distance is proportional to a dimensionless storage term, $r_r/r_w \propto \sqrt{\pi r_c^2/\pi r_w^2 S}$, where r_r is the maximum distance traveled by a specified fraction of the initial excess head over the duration of the slug test, r_w is the radius of the well bore, r_c is the radius of the well casing, S is the storage coefficient, and πr_c^2 is the well bore storage. The range of the slug test thus grows as the storage coefficient shrinks.

[5] These results suffer from three basic limitations. First, the range of a slug test is often defined in terms of an arbitrary fraction of the initial excess head; e.g., 1%, 5%, or 10%. Second, most analyses ignore the effects of heterogeneity and are performed in homogeneous systems, or

0043-1397/02/2001WR001072

systems with idealized heterogeneities (e.g., annular heterogeneities or low-permeability skins). Third, the range does not provide information about the relatively greater influence on the measured properties of the subsurface near the well compared to those of the subsurface farther away from the well.

[6] *Harvey* [1992] conducted Monte Carlo simulations of slug tests in three-dimensional realizations of random hydraulic conductivity fields to find the radius of a cylinder around the well, and the power averaging within the cylinder, that gave the best agreement between the estimated conductivity from the slug test and that computed by volume averaging within the cylinder. He found that: (1) The volume measured by a slug test was well approximated by $r_c/\sqrt{S}$, in agreement with the perturbation distance described above. (2) The type of averaging within the cylinder varied from near the geometric mean for two-dimensional systems, to larger values for some three-dimensional systems. (3) Conductivity estimates obtained simultaneously with specific storage estimates reflected the actual conductivity within a much larger volume than when the conductivity was estimated alone by specifying the specific storage to the true value. (4) Estimated specific storage values reflected near-well conductivity values, and hence were quite variable and biased to be larger than the true specific storage values because of larger effective conductivity near the well. These results were all predicated on the assumption that the slug-test estimated parameters are affected equally by all conductivity values within a cylinder of finite radius, but abruptly insensitive to conductivity beyond this radius. Our analysis, based upon a spatial filtering approach, addresses the limitations of earlier studies. The essential contribution we make is to determine the spatial filter functions that best reproduce the transmissivity and storage determined by analyzing slug-test data with a simple homogeneous-parameter model.

[7] Our paper begins with a review of the spatial filtering concept and how it applies to hydraulic well testing. We then discuss the numerical methods we use to simulate slug tests and determine the spatial filter functions. We first present filter functions computed using a sensitivity method in systems with homogeneous parameters. We show that the support volume of the filter function, and therefore the scale of a slug test, depends upon the storage parameter $\sqrt{\pi r_c^2/\pi r_w^2 S}$. We next use a deconvolution approach to examine systems with heterogeneous aquifer transmissivity and spatially uniform storage coefficient. We investigate a spatial power law filter for heterogeneous transmissivity fields, and the effect of heterogeneity length scales upon the value of the power exponent. We do not consider the case of spatially heterogeneous storage coefficient. Indeed, storage properties are thought to be less variable than transmissivity [*Dagan*, 1989, p. 163], and the head in the slug well is much less sensitive to aquifer storage than to transmissivity [*McElwee et al.*, 1995a].

2. Methodology

[8] We use a simulation approach to investigate the relationship between smaller-scale hydraulic parameters and the parameters that are measured by a slug test. We simulate slug test data in homogeneous and heterogeneous systems using a two-dimensional numerical flow model, which we call the aquifer model. We determine slug-test measured hydraulic parameters by fitting the aquifer model data with a one-dimensional uniform-parameter slug-test model. We relate the parameters of the two-dimensional aquifer model (small-scale parameters) to the slug-test measured parameters using a spatial filter.

2.1. Spatial Averaging Under Steady Radial Flow

[9] The approach we take follows closely upon the work of *Desbarats* [1992], who examines the spatial averaging of transmissivity under conditions of steady state, two-dimensional radial flow toward a well, such as occurs during a constant discharge test. Motivated by bounds derived by *Cardwell and Parsons* [1945], *Desbarats* [1992] proposes a weighted geometric spatial average T_{A_r} over a region A as an approximation for the effective transmissivity in that region:

$$\ln T_{A_r} = \frac{1}{W_A}\int_A \frac{y(x)}{r^2(x)}dA, \tag{2.1}$$

where x is the spatial coordinate, $y(x) = \ln T(x)$ is log transmissivity and for a region of area of A, $W_a = \int_A \frac{dA}{r^2(x)}$. *Desbarats* [1992] defines the effective transmissivity as that transmissivity determined by the analysis of drawdown in the pumping well using either one of two simple analytical radial flow models. In a set of numerical Monte Carlo experiments, the transmissivity determined using the spatial averaging formula provides excellent agreement with both effective transmissivities.

[10] To extend these results to three-dimensional flow, *Desbarats* [1994] introduces a generalized weighted power average of hydraulic conductivity K_V, as an approximation for the effective conductivity K_E determined by the analysis of drawdown from a steady state constant discharge test,

$$K_V^\omega = \frac{1}{W}\int_V \frac{\kappa^\omega(x)}{r^2(x)}dV, \tag{2.2}$$

where V is a drainage region, ω is a power exponent, κ is the hydraulic conductivity and $W = \int_V \frac{dV}{r^2(x)}$. The essential difference between (2.1) and (2.2) is the power exponent ω, which accounts for dimensionality effects. By expanding κ^ω in a Taylor series, *Desbarats* [1994] approximates (2.2) by

$$\ln K_V \approx \psi_V + \frac{\omega}{2}\frac{1}{W}\int_V \frac{(\psi(x)-\psi_V)^2}{r^2(x)}dV, \tag{2.3}$$

where $\psi(x) = \ln \kappa(x)$ and $\psi_V = \frac{1}{W}\int_V \frac{\psi(x)}{r^2(x)}dV$. This relationship allows *Desbarats* [1994] to develop a geostatistical model that relates the effective conductivity of the drainage region to the conductivity at the well.

2.2. Spatial Filtering Approach

[11] Similar to *Desbarats* [1992, 1994], we conceive of a slug-test measured parameter, $Z(x)$ (either storage S or transmissivity T) to be a weighted spatial average of $z(x)$,the corresponding parameter defined at a smaller scale. This weighted spatial averaging can be mathematically represented as a spatial-filtering operation [*Beckie*, 2001],

$$Z^\omega(x) = \int_V \mathcal{G}(x-x')z^\omega(x')dx', \tag{2.4}$$

here written as a nonlinear filter using a power exponent ω. The value of the filter function $\mathcal{G}$ is the weight given to the smaller-scale property in the spatial average. The support volume can be thought of as that volume where the filter function has significant weight. In this framework, (2.1) and (2.2) can be viewed as linear and power-average spatial filters where the parameters defined at a smaller scale, y and κ^{ω} are filtered with filter functions that decay as r^{-2} away from the well. In (2.4) and (2.2), the smaller-scale properties are averaged arithmetically when $\omega = 1$, harmonically when $\omega = -1$ and geometrically when $\omega \rightarrow 0$.

[12] Because the hydraulics of slug-tests are transient, our analysis differs from Desbarats' analysis of steady state flow to a well in that we must consider both the estimates of T and S, and the potential relation between these estimates. In addition, for the slug test T and S can only be estimated through an inverse procedure whereas transmissivity and conductivity can be directly estimated using the steady state analytical models for two- and three-dimensional radial flow, respectively.

[13] Following *Desbarats* [1994], we also consider an approximation of (2.4) that relates smaller-scale transmissivity to T_{meas} the transmissivity determined by the inversion of slug test data,

$$\ln T_{meas} \approx Y_V + \frac{\omega}{2} S_V^2, \tag{2.5}$$

where $Y_V = \int_V \mathcal{G}(x - x')y(x')dx'$ is a spatially averaged log transmissivity, and $S_V^2 = \int_V \mathcal{G}(x - x')(y(x') - Y_V)^2 dx'$ is a spatially filtered variance of log transmissivity [see *Desbarats*, 1994, equations (10)–(13)]. This approximation of the nonlinear filter (2.4) can be used to develop a geostatistical model such as described by *Desbarats* [1994] (note that the approximation is linear in ω but nonlinear, through the $S^2{}_V$ term, in log transmissivity). We do not pursue a geostatistical model in this paper, but show later that the values of the power exponent determined using the approximation (2.5) agree closely with those determined using the nonlinear filter (2.4).

2.3. Slug-Test Models

[14] The most common analytic models used to interpret slug tests are the *Hvorslev* [1951], the *Bouwer and Rice* [1976], and the *Cooper et al.* [1967]. The properties, application and extension of these basic models are presented by a number of authors [*Barker and Black*, 1983; *Bouwer*, 1989; *Brown et al.*, 1995; *Butler and Healey*, 1998; *Butler et al.*, 1996; *Chirlin*, 1989; *Dagan*, 1978; *Dax*, 1987; *Demir and Narasimhan*, 1994; *Faust and Mercer*, 1984; *Harvey*, 1992; *Hyder and Butler*, 1995; *Hyder et al.*, 1994; *Karasaki et al.*, 1988; *McElwee et al.*, 1995a, 1995b; *Moench and Hsieh*, 1985; *Novakowski*, 1989; *Pandit and Miner*, 1986; *Peres et al.*, 1989; *Ramey et al.*, 1975; *Sageev*, 1986; *Wang*, 1995; *Widdowson et al.*, 1990; *Yang and Gates*, 1997; *Zlotnik*, 1994]. We focus on slug tests in perfectly confined aquifers with fully penetrating wells. *Chirlin* [1989] reviews the applicable models and concludes that the *Cooper et al.* [1967] method most accurately represents the physical processes. In particular, the *Bouwer and Rice* [1976] and *Hvorslev* [1951] models employ approximations to account for the effects of elastic storage [*Brown et al.*, 1995; *Chirlin*, 1989; *Demir and Narasimhan*, 1994]. Accordingly, we use the *Cooper et al.* [1967] slug-test model as the basis for our analysis of slug tests in perfectly confined aquifers with fully penetrating wells.

[15] The *Cooper et al.* [1967] slug-test model is defined by the following boundary-value problem,

$$\nabla \cdot (T \cdot \nabla h) = S\frac{\partial h}{\partial T}, r \geq r_w, \tag{2.6}$$

$$\int_0^{2\pi} T\frac{\partial h}{\partial r} r d\theta = \pi r_c^2 \frac{dH_{wb}}{dt}, r = r_w, \tag{2.7}$$

$$h(r_w, t) = H_{wb}(t), \tag{2.8}$$

$$H_{wb} = H_{wb}(0), t = t_0, r = r_w \tag{2.9}$$

where h is the hydraulic head, H_{wb} is the head in the well bore $H_{wb}(0)$ is the initial excess head and t, r, and θ are time, radial and angular coordinates. *Jaeger* [1940, 1955] first published analytic solutions for these equations, which in his case are applied to thermal slug tests that are used to estimate thermal conductance and heat capacity of the ocean floor. *Cooper et al.* [1967] then introduced the solution to the groundwater literature.

2.4. Filter Function Identification

[16] In this work, we first identify the filter function $\mathcal{G}$ using a sensitivity approach, and then identify the power exponent ω using a deconvolution method [*Beckie*, 2001]. While it may be theoretically more desirable to estimate both simultaneously, we find that a two-step approach is more practically implemented. Indeed, we first determine the filter function $\mathcal{G}$ for the case when the smaller-scale transmissivity field is spatially homogeneous. The identified filter function $\mathcal{G}$ then can be thought of as the function that is applicable to the case of weak heterogeneities in a homogeneous background. Note that when the smaller-scale field is homogeneous, the power exponent ω has no effect and can be set to one. We show later that the filter function identified using homogeneous properties can be applied to transmissivity fields with strong heterogeneities (S_Y^2 up to 7.9).

[17] We use a deconvolution (or regression) method to determine the power exponent ω for heterogeneous fields. To do this, we fix the filter function to the function identified in the previous step using the sensitivity method with homogeneous parameters. We assume that ω is dependent upon the correlation structure of the underlying smaller-scale parameter field, but that the filter function $\mathcal{G}$ is independent of this structure. Later, we evaluate these assumptions a posteriori by cross plotting slug-test measured parameters against those parameters determined using the spatial filter expression.

[18] In application of the spatial filters to field estimation problems, the detailed structure of the smaller-scale parameter field will not be known. In that situation, one can only hope that the spatial filter is relatively insensitive to the unknown details of the parameter fields. We show later that this appears to be true for relatively unstructured hetero-

geneity. Large-scale organized heterogeneities, such as high conductivity channels or fractures, are often revealed in the head-recovery data, which deviates very strongly from a homogeneous-aquifer (ideal) response. If a strongly non-ideal response is observed, it would be imprudent to attempt to interpret the data with a homogeneous-parameter model, or to apply a spatial filter based upon such a model.

2.4.1. Sensitivity Method

[19] The sensitivity method that we use is presented by *Beckie* [2001], so we provide only a brief description here. We must define: (1) the smaller-scale model that we use to simulate the real-world slug-test, (2) the larger-scale model that we use to interpret the slug-test data, and (3) how we determine the larger-scale model parameters that best fit the slug-test data (the inverse method).

[20] We simulate slug-test head recovery data numerically in two-dimensional aquifers with either homogeneous or heterogeneous parameters. We solve the boundary value problem given by equations (2.6)–(2.9) using a numerical method that we describe later. We call this the smaller-scale model or the aquifer model, and denote the head solution $h(x, t; \mathbf{z})$, where h is the small-scale head and $\mathbf{z}$ is a $2nb \times 1$ vector of aquifer-model parameters (e.g., transmissivity and storage in each of nb gridblocks of a numerical model).

[21] We interpret the head-recovery data with what we call the slug-test model or larger-scale model. This model is again given by equations (2.6)–(2.9), now, however, with T and S spatially uniform. We denote the solution to this model $H(x, t; \mathbf{Z})$, where H is the large-scale head, and $\mathbf{Z}$ is a 2×1 vector of slug-test model parameters.

[22] If we specify the small-scale model parameters $\mathbf{z}$, then we can simulate the head recovery in the well at nt time steps $h(x_w, t_i; \mathbf{z})$, $i = 1,\ldots,nt$, where x_w is the position of the well and t_i is the time at the end of time step i. We can then determine slug-test measured parameters from the head-recovery data as the parameters $\mathbf{Z}$ that minimize the following least squared error objective function,

$$(\mathbf{h} - \mathbf{H}(\mathbf{Z}))^T \mathbf{W} (\mathbf{h} - \mathbf{H}(\mathbf{Z})), \tag{2.10}$$

where $\mathbf{h}$ is an $nt \times 1$ matrix containing the well bore head computed at nt times using the smaller-scale model with parameters $\mathbf{z}$, and $\mathbf{H}(\mathbf{Z})$ is a $nt \times 1$ matrix containing the well bore head computed at nt times using the slug-test model with parameters $\mathbf{Z}$, $\mathbf{W}$ is a weighting matrix and superscript T indicates matrix transpose. In this paper, all results are obtained with the weighting matrix set to the identity matrix, and with time steps separated by equal intervals of log time.

[23] As we employ numerical models, it is appropriate to develop a discrete, finite-dimensional filter relating the $2nb \times 1$ vector of smaller-scale parameters $\mathbf{z}$ to the 2×1 vector of slug-test measured parameters $\mathbf{Z}$. Such a filter is written with a $2 \times 2nb$ filter matrix $\mathbf{G}$

$$\mathbf{Z} = \mathbf{G}\mathbf{z}, \tag{2.11}$$

(see equation (2.4)). As we consider power averages of transmissivity and not storage coefficient, it is convenient to use transmissivity to the power ω and storage coefficient in (2.11), such that $z = \left\{ {\tau^\omega \atop s} \right\}$ and $Z = \left\{ {T^\omega \atop S} \right\}$, where τ and s are transmissivity and storage coefficient defined at the smaller scale. For the case of geometric averaging of transmissivity, filter matrix then can be partitioned into 4 submatrices $\mathbf{G} = \begin{bmatrix} G_{YY} & G_{YS} \\ G_{SY} & G_{SS} \end{bmatrix}$. Each submatrix can be interpreted as an nb-gridblock discretization of a filter function relating parameters from the gridblocks of the smaller-scale model to the slug-test-measured parameters. For example, G_{SY} relates smaller-scale log transmissivity to the slug-test measured storage coefficient.

[24] Using a sensitivity approach, *Beckie* [2001] develops an expression for $\mathbf{G}$ in (2.11) for the case when the power exponent ω is equal to one,

$$\mathbf{G} = \left[\mathbf{F}^T \mathbf{W} \mathbf{F}\right]^{-1} \mathbf{F}^T \mathbf{W} \mathbf{f}. \tag{2.12}$$

where $[\mathbf{F}]_{ij} = [\partial H(x_w, t_i; Z_b)]/(\partial Z_j)$ and $[\mathbf{f}]_{ij} = [\partial h(x_w, t_i; z_b)]/(\partial z_j)$ are the slug-test and aquifer model sensitivities. The value of $[\mathbf{G}]_{ij}$ can be interpreted as the influence of a perturbation in the value of an aquifer model parameter z in gridblock j from some base-case upon the slug-test model parameter Z_i. We determine the model sensitivities $\mathbf{f}$ and $\mathbf{F}$ in the filter expression (2.12) using the discrete adjoint-state theory of *Townley and Wilson* [1985]. We verify the derivatives by comparison to brute-force finite differences and to the results of *McElwee et al.* [1995a]. Having determined the filter function $\mathbf{G}$ using a sensitivity method, we next determine the power exponent ω using a deconvolution approach.

2.4.2. Deconvolution Method

[25] We first generate an ensemble of smaller-scale log transmissivity fields having a specified statistical structure. We then simulate slug-test head recovery data in each realization using the numerical methods described in the next section. We then invert the head recovery data as described above (equation 2.10), to yield Y_{meas} and S_{meas}, the slug-test measured log transmissivity and storage. For each ensemble of smaller-scale log transmissivity fields, we determine one power exponent ω for the nonlinear filter expression (2.4) and one value of ω for the linearize filter expression (2.5).

[26] To determine ω for the nonlinear filter expression (2.4), we fix the filter functions $\mathbf{G}$ to those that we determined using the sensitivity method with homogeneous parameters, and then choose that ω which minimizes the fitting error in the specified ensemble of realizations

$$\sum (Y_{meas} - Y(\omega))^2, \tag{2.13}$$

where $Y(\omega)$ is the log transmissivity determined using the spatial filter (2.11) and the sum is over all members of the ensemble. We evaluate the derived filter a posteriori by cross plotting Y_{meas} versus $Y(\omega)$ for several values of ω, including the optimal value, which is the value of ω that minimizes (2.13).

[27] To determine ω for the approximate filter expression (2.5), we follow the approach described by *Desbarats* [1994]. For each realization of log transmissivity from an ensemble of fields, we compute the log transmissivity spatial average Y_V and variance S_V^2 and substitute them into the approximate filter expression (2.5), along with the log transmissivity determined for that realization by fitting the

recovery data using (2.10), and solve for ω. We average the values of ω over all realizations to define the optimal value for the ensemble.

2.5. Numerical Methods

[28] We discretize the aquifer flow model using a standard radial-coordinate, implicit in time, finite-volume approach, similar to that used by *Brown et al.* [1995]. We place the nodes within the gridblocks according to the geometry embedding theory of *Narasimhan* [1985]. The well bore is simulated as gridblocks with transmissivity 5 orders of magnitude larger than the highest values found in the mesh and a storage coefficient of r_c^2/r_w^2. In addition, we compute inter-gridblock conductances using the averaging approach also presented by *Narasimhan* [1985]. In all simulations in this paper, the grid has 81 gridblocks in the angular direction and 81 gridblocks in the radial direction. The radial dimension of the gridblocks grows geometrically away from the well bore such that $\Delta r_i = a\Delta r_{i-1}$, where Δr_i is the radial dimension of gridblock i, with i increasing away from the borehole, and where a is a geometric factor, which depends upon the storage coefficient. Constant-head boundary conditions are assigned to the outer boundary. For each value of storage, trial and error simulations were used to determine an appropriate position for the outer boundary (and the value of the factor a) such that when the constant head boundary condition is replaced by a zero-flux condition, the head in the well bore changes by less than 1 part in 10,000 at any time step.

[29] We also numerically solve the one-dimensional *Cooper et al.* [1967] model with spatially homogeneous parameters (our so-called slug test model). We use the slug-test model to invert the head recovery data generated from the aquifer model and thus determine the slug-test measured parameters. We use a high accuracy one-dimensional radial discretization, a fine time discretization and the same finite-volume method with geometry embedding and grid blocks that grow in size away from the well bore that we use for the aquifer model.

[30] We generate heterogeneous log transmissivity fields for the radial grids using a method described in Appendix A. With variable-sized gridblocks in the radial mesh, it is not possible to avoid complex support-scale effects when generating the fields. When gridblock sizes vary, geostatistics such as integral scale and spatial variance are not well defined. Accordingly, the correlation properties of the generated fields only approximate the target values of the corresponding single-support scale fields. Nevertheless, the relative magnitude of correlation properties of the single support-scale fields should be preserved using our methods and should therefore not affect our conclusions about the role of correlation scale on the value of the power exponent ω.

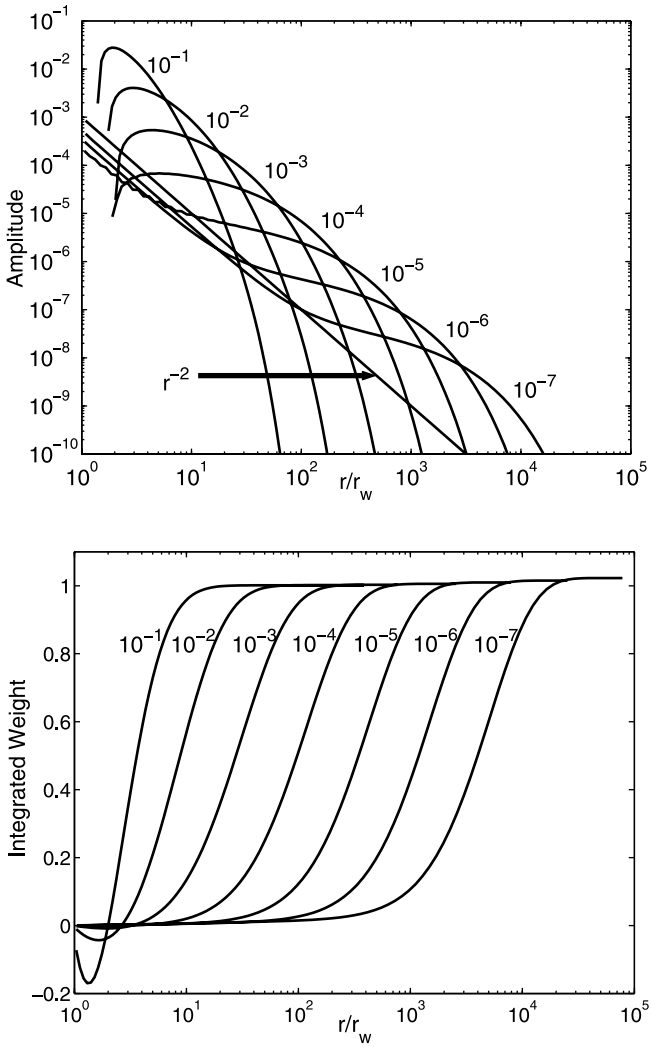

Figure 1. The *YY* filter functions, which show how small-scale log transmissivity is averaged by slug-test estimated log transmissivity. The filters are symmetric with angle θ around the pumping well, so only a profile is shown here. Each filter is labeled by the storage coefficient used to determine the filter. (a) Amplitude of the filter function plotted versus dimensionless radial distance from the well, r/r_w. Negative values at small radius for the $S = 10^{-1}$,10^{-2},10^{-3} and 10^{-4} filters are not plotted on the log scale. An r^{-2} trend line is also plotted. As storage decreases the filters approach the steady state r^{-2} behavior presented by *Desbarats* [1992]. (b) Integrated filter weight, $\int_{r_w}^{r} \mathcal{G}(r')2\pi r' dr'$ versus dimensionless radial distance from the well.

3. Results

3.1. Homogeneous Aquifer

[31] We first present the filter functions determined when the two dimensional aquifer is homogeneous. The homogeneous-parameter filter functions are symmetric with respect to the angular coordinate direction and thus are plotted versus dimensionless radial distance r/r_w. The *YY*, *SS*, *SY*, and *YS* filter functions are plotted in Figures 1–4 Part "a" of each figure shows the filter amplitude and part b shows integrated filter weight, where the integrated weight at distance r is equal to $\int_{r_w}^{r} \mathcal{G}(r')2\pi r' dr'$. In each figure, we label the filter functions with the storage coefficient used to determine the function. The *YS* filter functions have been made dimensionless by multiplying by $-S/\log_{10}T$ and *SY* filter functions have been made dimensionless by multiplying by $\log_{10}T/S$.

[32] The support volume of the slug test can best be appreciated by examining the integrated filter weights in the "b" panels of Figures 1–4. The range of the slug test is that

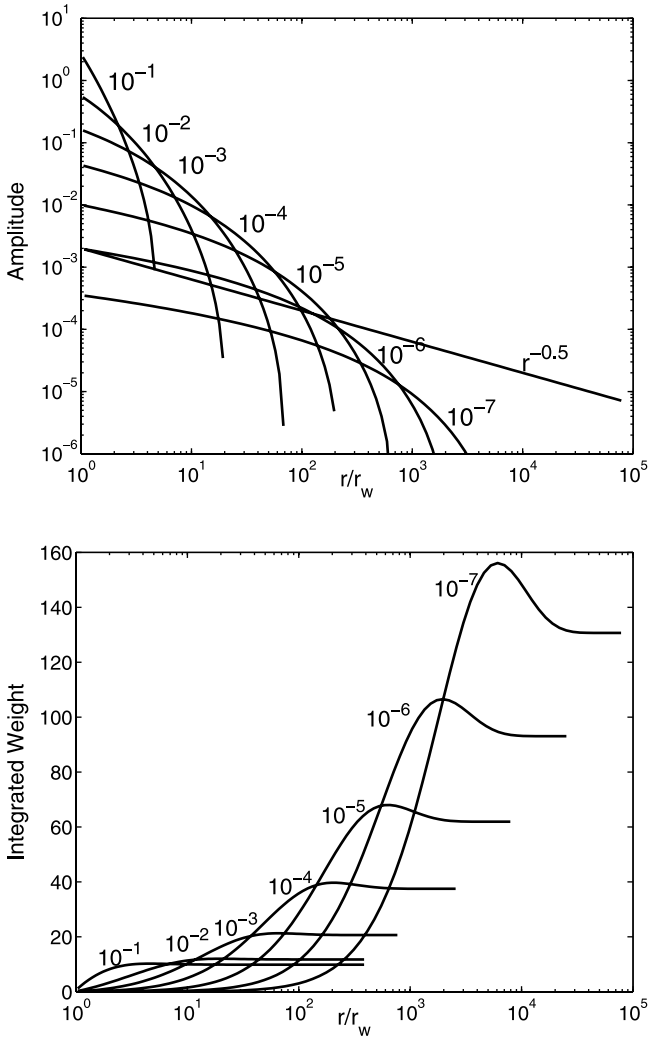

Figure 2. The *SS* filter functions, which show how small-scale storage coefficient is averaged by slug-test estimated storage coefficient. The filters are symmetric with angle θ around the pumping well, so only a profile is shown here. Each filter is labeled by the storage coefficient used to determine the filter. (a) Amplitude of the filter function plotted versus dimensionless radial distance from the well, r/r_w. An $r^{-0.5}$ trend line is also plotted. (b) Integrated filter weight, $\int_{r_w}^{r} \mathcal{G}(r')2\pi r' dr'$ versus dimensionless radial distance from the well.

distance where the integrated weight reaches a constant plateau at large r/r_w. The subsurface outside of that range does not affect the parameter measured by the slug test. In Figure 5 we plot the ranges of the *YY* filter versus $S^{-0.5}$. We also plot from *Guyonnet et al.* [1993] the distances at which a head perturbation at the well dissipates to either 1% or 5% of its initial value. The slug-test range is bounded by these two dissipation distances.

[33] The total integrated weight of the filter indicates whether there is bias in the slug-test parameter estimation. The plateau values of the *YY* filter functions (Figure 1b) are between 1.001 and 1.004, indicating that these filters are essentially mean preserving.

[34] It is interesting that as the storage coefficient decreases, the *YY* filter functions in Figure 1 approach the r^{-2} weighting proposed by *Desbarats* [1992] for steady state flow conditions. However, near the well bore at $r/r_w = 1$, the *YY* filter functions for $S = 10^{-1}$, $S = 10^{-2}$, $S = 10^{-3}$ and $S = 10^{-4}$ take on negative values, which are not plotted in Figure 1a (because of the logarithmic scale) but are apparent in Figure 1b.

[35] The negative values of the *YY* filter function (Figure 1) near the well result from the interaction between estimated transmissivity and storage. We can demonstrate this by computing *YY* filter functions with storage fixed and known, in contrast to all other results in this paper, where both storage and transmissivity are inverted from the recovery data. If we know storage, then we set to zero the storage sensitivities in

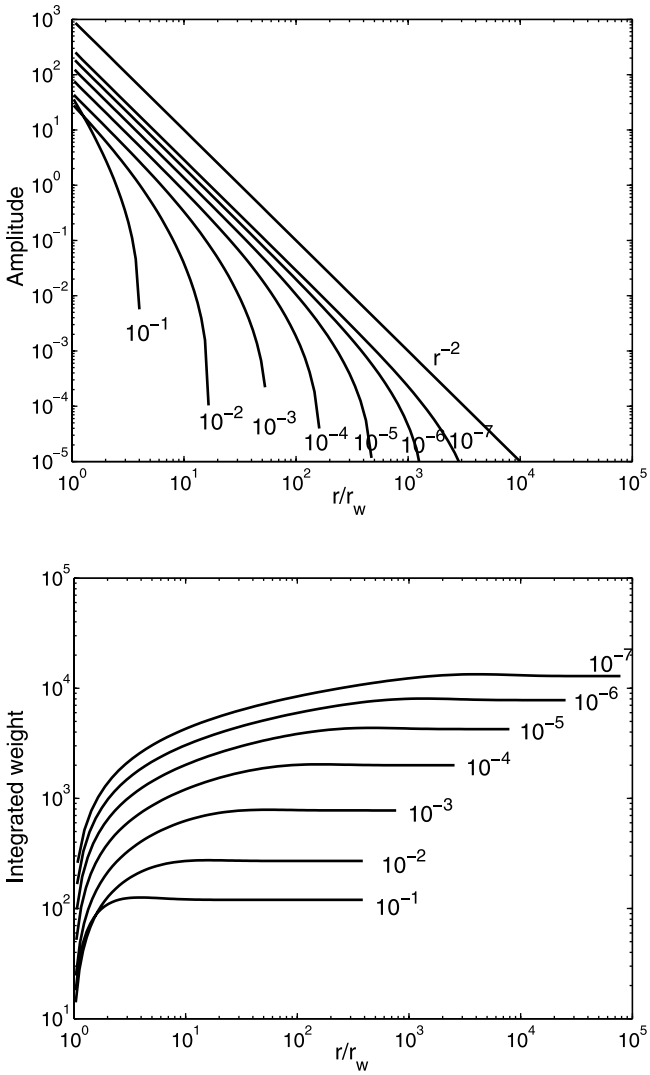

Figure 3. The *SY* filter functions, which show how small-scale transmissivity affects slug-test estimated storage coefficient. The filters are symmetric with angle θ around the pumping well, so only a profile is shown here. Each filter is labeled by the storage coefficient used to determine the filter and have been normalized by multiplying by $\log_{10}T/S$. (a) Amplitude of the filter function plotted versus dimensionless radial distance from the well, r/r_w. An r^{-2} trend line is also plotted. (b) Integrated filter weight, $\int_{r_w}^{r} \mathcal{G}(r')2\pi r' dr'$ versus dimensionless radial distance from the well.

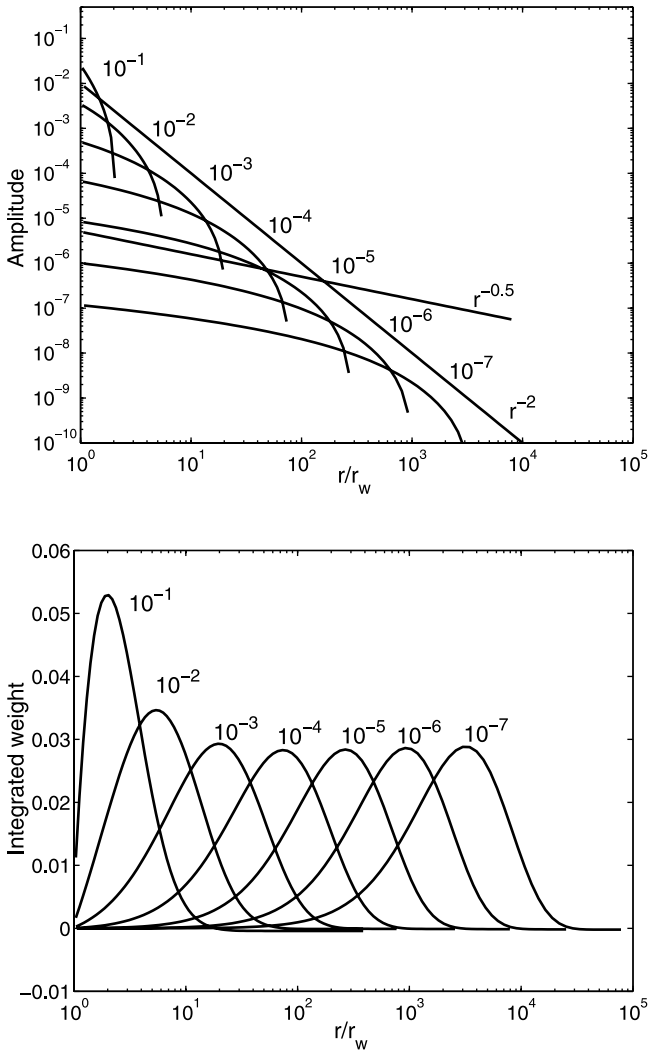

Figure 4. The *YS* filter functions, which show how small-scale storage affects slug-test estimated transmissivity. The filters are symmetric with angle θ around the pumping well, so only a profile is shown here. Each filter is labeled by the storage coefficient used to determine the filter and have been normalized by multiplying by $-S/\log_{10}T$. (a) Amplitude of the filter function plotted versus dimensionless radial distance from the well, r/r_w. Trend lines of $r^{-0.5}$ and r^{-2} are also plotted. (b) Integrated filter weight, $\int_{r_w}^{r} \mathcal{G}(r')2\pi r' dr'$ versus dimensionless radial distance from the well.

(2.12). The resulting known-storage filter functions are shown in Figure 6. The filters are positive everywhere and follow an almost exact r^{-2} behavior, corresponding to the filters used by *Desbarats* [1994]. Indeed, the negative values of the *YY* filter function cannot be explained if log transmissivity alone were to contribute to the slug-test measured log transmissivity. It would imply that where the filter is negative, a more conductive zone would lead to a lower estimated transmissivity. In field settings, the storage is not known a priori, and hence the filters computed assuming fixed storage are not appropriate. Later in the paper, we show how these parameters interact in the inverse procedure by analyzing a two-zone slug-test model.

[36] In Figure 2b the plateau values of the *SS* filter functions are all greater than one, indicating a bias in the slug-test estimate of storage from head-recovery data. The bias increases as the storage coefficient decreases. These results can be interpreted to say that small-scale deviations in storage from some base-case value are amplified in the storage value estimated from slug-test data. Similarly, the dimensionless *SY* filters in Figure 3, which describe the effects of small-scale transmissivity on the measured storage coefficient, show a very strong influence of transmissivity on storage. We show later that high values of transmissivity are associated with anomalously high values of storage, and low values of transmissivity are associated with anomalously low values of storage.

[37] The influence of storage on the measured log transmissivity is shown in *YS* filters (Figure 4). These filters integrate to essentially zero (Figure 4b), indicating that small-scale storage has a relatively weak net effect on measured transmissivity value.

3.2. Heterogeneous Aquifer

[38] In this section we examine how well the nonlinear power average filter expression, (2.4) and its approximation (2.5) predict log transmissivity values measured by an analysis of slug test data. We also investigate the relationship between the power averaging exponent ω and the integral scale of the smaller scale log transmissivity field.

[39] We analyze 73 different ensembles of log transmissivity fields, each ensemble with a specified statistical structure and containing at least 80 realizations. Realizations on a radial grid are generated as described in the appendix from single-support scale source fields that are defined on a rectangular grid. All the single-support scale fields are in turn generated with isotropic exponential

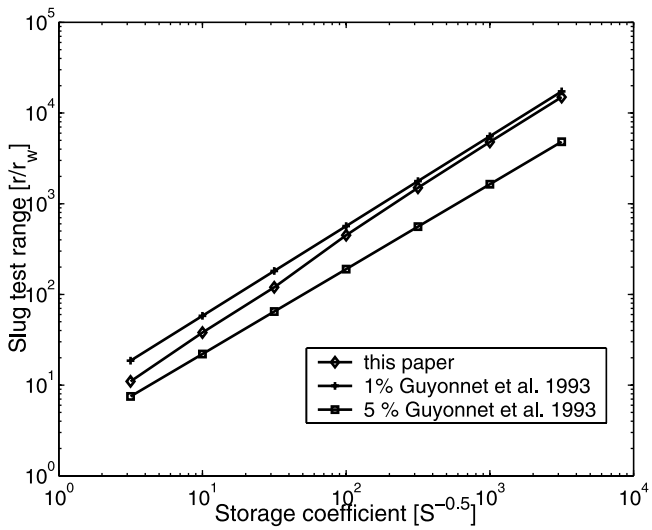

Figure 5. The slug test range versus radial distance from the well, where the range is defined in two ways: as the distance a specified percentage of the initial perturbation in the slugged well travels according to *Guyonnet et al.* [1993] and as the distance where the integrated weight of the filter function plateaus to a constant value (Figure 1b).

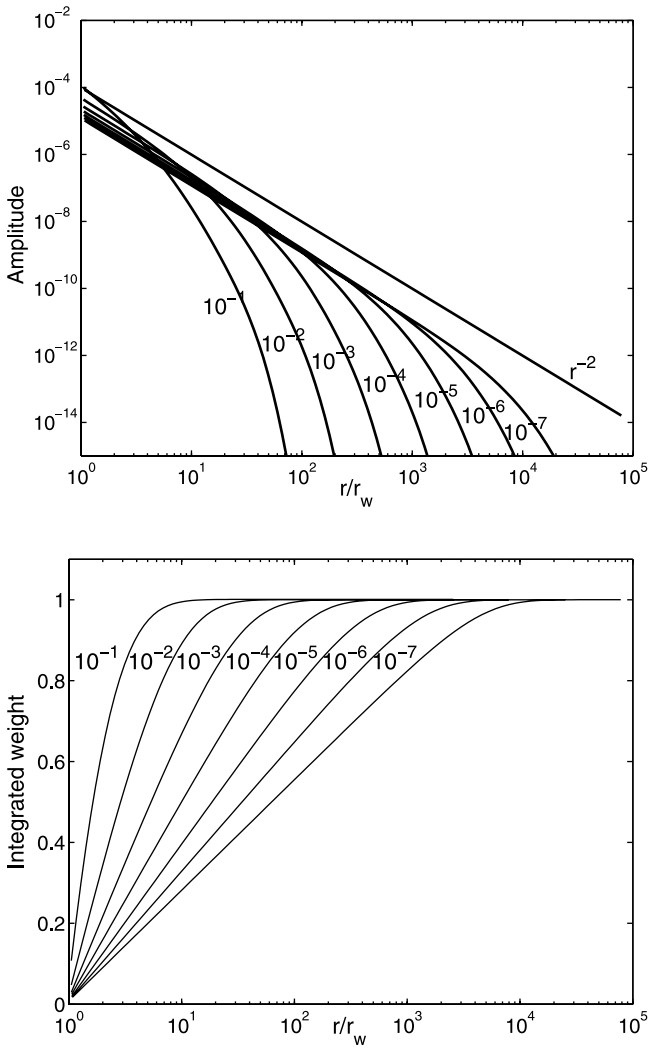

Figure 6. The *YY* filter functions here computed for the case where storage coefficient is fixed and known (cf. Figure 1). (a) Amplitude of the filter function plotted versus dimensionless radial distance from the well, r/r_w. An r^{-2} trend line is also plotted. (b) Integrated filter weight, $\int_{r_w}^{r} \mathcal{G}(r')2\pi r' dr'$ versus dimensionless radial distance from the well.

covariance functions that have specified integral scale λ and variance σ_Y^2. The integral scale that we assign to each radial-grid ensemble is the one used to generate the single-support scale source realizations. In the results that follow, we report λ/r_a, the integral scale normalized by the range of the filter function r_a, which is plotted in Figure 5 and depends only upon the value of the storage coefficient and the well bore storage. Storage coefficient values that we use range from 10^{-1} to 10^{-5} (Table 1).

[40] In Figure 7 we plot transmissivity measured by the inversion of slug test response data with the Cooper-Bredehoeft-Papodopolus model (the "true" slug-test transmissivity) versus the transmissivity predicted with the spatial filtering expression (2.4) using the optimal power exponent ω and the filter function corresponding to the storage value used to simulate the slug tests. Table 1 provides some of the statistical properties of the corresponding ensembles. The value of normalized integral scale λ/r_a increases from $\lambda/r_a = 0.06$ in Figure 7a to $\lambda/r_a = 35.0$ in Figure 7f.

[41] We find that the power exponent is a function of the normalized integral scale of the log transmissivity field, λ/r_a. In Figure 8 we plot the power exponent ω versus the normalized integral scale λ/r_a for all 73 ensembles, where each point represents at least 80 realizations. For values of normalized integral scale less than 0.1, the power exponent is approximately between -0.19 and -0.1, indicating dominantly geometric averaging (i.e., $\omega = 0$). As λ/r_a grows, the power exponent grows to a maximum of $\omega = 0.35$. There is considerable scatter at larger values of λ/r_a.

[42] The sensitivity of the fits to the value of the power exponent can be seen in Figure 9, which shows the measured transmissivity plotted versus the transmissivity predicted with the spatial filtering expression (2.4) using several values of the power exponent ω, including the optimal value. These plots show data from the same realizations as found in Figure 7. The plots show a strong effect of the power exponent on the fit when the normalized integral scale is small. At large values of the integral scale (e.g., Figure 9f), the power exponent has little effect, as indicated by relatively good fits at all values of ω. Figure 10 is a cross plot of the power exponent computed using the approximate filter (2.5) and the filter (2.4). The figure shows a very good correspondence between the power exponent computed for the approximate filter and the nonlinear filter. This suggests that the computed power exponents are not strongly affected by fitting artifacts, since the power exponent was determined in a different way for each filter.

4. Storage-Transmissivity Interaction

[43] A surprising result in Figure 1 is the negative values of the log transmissivity filter function when the storage coefficient is large. Here we examine the interaction between storage and transmissivity near the well bore by comparing late-time approximations of the analytical solution of the *Cooper et al.* [1967] model (homogeneous parameters) with that of the finite skin thickness slug-test model of *Moench and Hsieh* [1985] (two-zone model). We develop the Laplace domain late time approximations to these models in Appendix B, equations (8.7) and (8.8). The *Moench and Hsieh* [1985] model includes a finite thickness skin of transmissivity T_1 that extends to a radius r' from the well bore, beyond which the transmissivity has the value T_2.

Table 1. Statistics and Results for Ensembles Used to Produce Figures 7 and 10[a]

Ensemble	λ/r_a	S	ω_{opt}	$\sigma^2_{\ln T}$	S_Y^2
a	0.06	10^{-4}	−0.171	10.6	7.93
b	0.15	10^{-4}	−0.097	10.6	6.07
c	0.25	10^{-3}	−0.056	10.6	6.05
d	1.25	10^{-4}	−0.077	10.6	5.76
e	10.0	10^{-3}	+0.185	10.6	4.76
f	35.0	10^{-2}	+0.345	10.6	4.76

[a]Each ensemble contains a minimum of 80 realizations. $\sigma^2_{\ln T}$ is the spatial variance of the single support scale ensemble used to create the radial grid ln T fields (see Appendix A).

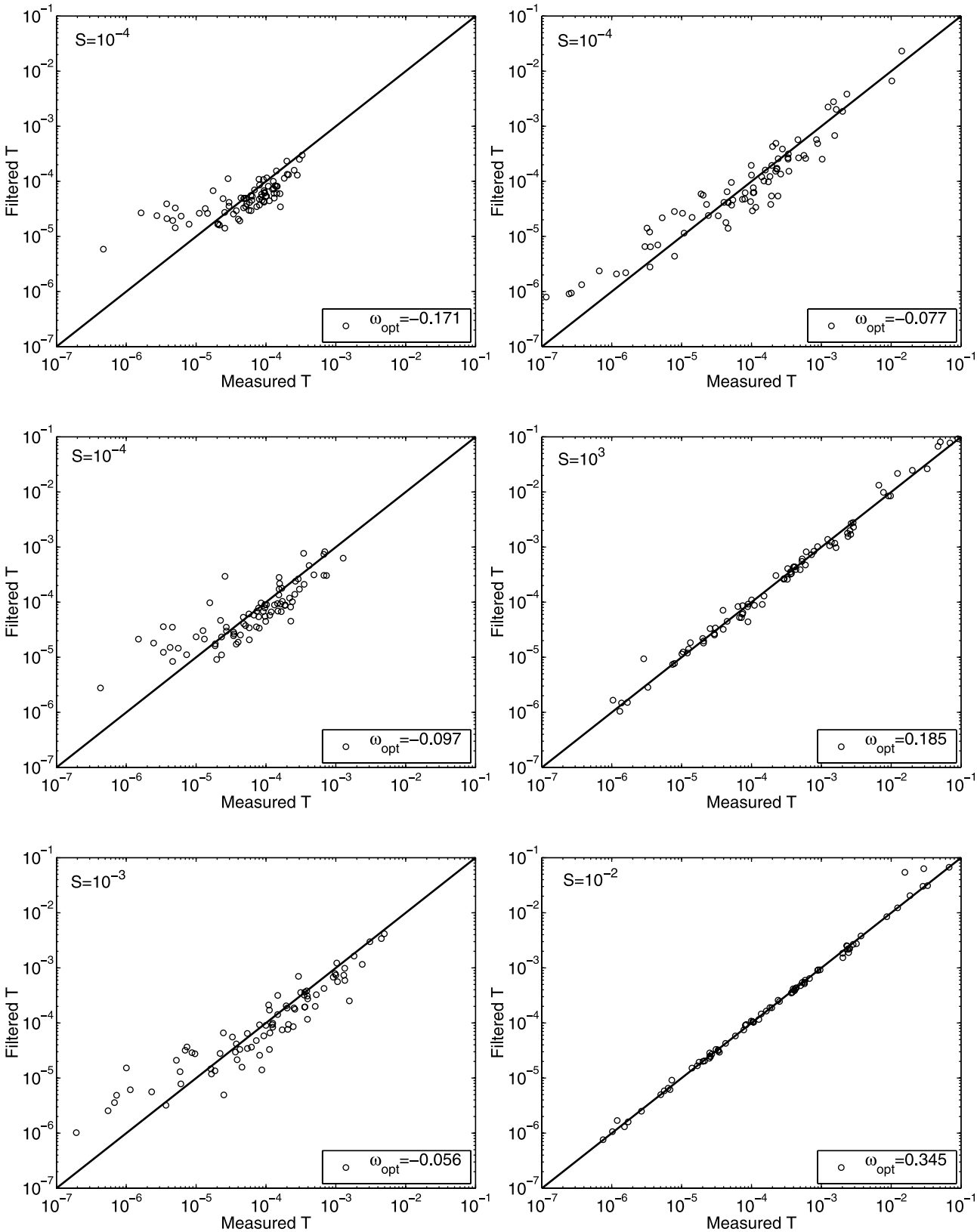

Figure 7. Cross plots of transmissivity estimated by analysis of slug-test recovery data (''true'' slug-test transmissivity) versus transmissivity computed using the power spatial filter. Each point corresponds to one realization of a random field, and each figure (a–f) corresponds to a different ensemble. Ensemble statistics and the storage coefficient used for the simulations are provided in Table 1.

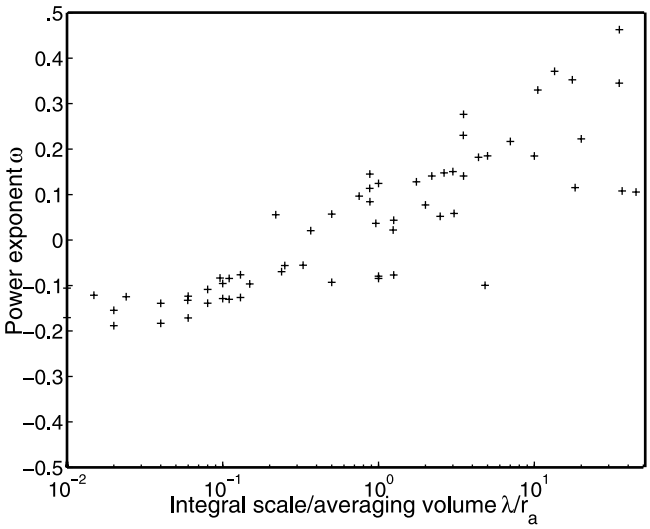

Figure 8. Power exponent versus the ratio of characteristic scale of heterogeneity to the scale of the averaging volume. Each point represents a power exponent determined from a minimum of 80 realizations.

[44] At late times, both models have the same basic form with the following correspondence:

Homogeneous parameters	Two zone
T	T_2
S	$S\left(\frac{r'}{r_w}\right)^{-2(T_2/T_1-1)}$

[45] Since the approximations (8.7) and (8.8) in Appendix B are of the same form, they can mimic each other. When the transmissivity near the well is lower than the transmissivity far from the well, the head response can be mimicked by a system with uniform transmissivity equal to the transmissivity far from the well and a much smaller storage coefficient. When the transmissivity near the well is higher than the transmissivity far from the well, the head response can be mimicked by a system with uniform transmissivity equal to the transmissivity far from the well and a large storage coefficient S.

[46] Our simulations show these two effects quite clearly. Figure 11 is a scatterplot of the storage coefficient versus transmissivity estimated from head response data using the *Cooper et al.* [1967] model with homogeneous transmissivity. The head response data is produced by simulations in heterogeneous transmissivity fields. The plotted storages and transmissivities come from a combination of a number of ensembles where the true storage coefficient is 10^{-4} and the estimated storage is bounded in the estimation routine to be between 10^{-9} and 10^{0}. As can be seen in Figure 11, low values of estimated storage coefficient are associated with low values of transmissivity and high values of estimated storage coefficient are predominantly associated with high values of transmissivity.

[47] The interaction between storage and transmissivity of the inner zone can be quantified using the late time approximations presented in Appendix B. If the homogeneous parameter model is used to analyze the late time solution of the two zone model, then the estimated S, denoted S_{est}, is related to the true S through the correspondence given above. Taking logarithms and rearranging, we have,

$$\ln(S_{est}) = \ln\left[S\left(\frac{r'}{r_w}\right)^2\right] - \frac{1}{T_1}\left[\ln\left(\frac{r'}{r_w}\right)^{2T_2}\right]. \qquad (4.1)$$

If r', r_w, and T_2 are kept fixed, then the above equation shows that $\ln(S_{est})$ is negatively correlated to $1/T_1$.

[48] This correlation explains the negative values of the spatial filters computed when both T and S are simultaneously estimated (Figure 1). When the head response is fit with both parameters free to vary, the storage value compensates for the transmissivity. It can be seen in Figure 1b that this effect is only significant for large storages and very near the well.

5. Discussion

[49] Our results in Figure 8 show that the power exponent depends upon the integral scale of the transmissivity field. However, Figure 9 shows that geometric averaging ($\omega = 0$) provides a good fit for all ensembles and for all storage values we examine between $S = 10^{-1}$ to $S = 10^{-7}$ (results not shown). Our results are in accord with the geometric averaging employed by *Desbarats* [1992], and consistent with well-established bounds for uniform radial flow in two dimensions [*Cardwell and Parsons*, 1945]. Indeed, *Desbarats* [1994] introduces the power exponent to account for three-dimensional flow effects. For two-dimensional transient flow considered here, a power exponent of $\omega = 0$ is probably adequate for most applications given the uncertainty in the value of λ/r_a, the integral scale of the transmissivity field. In situations where there are significant three-dimensional flow effects during the slug test then a power law filter may be necessary.

[50] We should note that we find no relationship between the power exponent and the spatially filtered variance of the log transmissivity field S_Y^2. In Table 1, S_Y^2 decreases with increasing integral scale λ/r_a. This trend can be explained by the approximate r^{-2} weighting in the definition of the spatially filtered variance. As λ/r_a increases, the field becomes smoother near the well, which receives the largest weight in the S_Y^2 computation. The realizations used for Figures 7 and 9, summarized in Table 1, are all strongly heterogeneous where the variances of the single-support scale fields are all $\sigma^2_{\ln T} = 10.6$.

[51] The shape of the filter function is primarily affected by the dynamics of the slug test and the inverse methodology. The quantity and type of fitting data and the number of parameters in the inverse procedure affect the filter function. In this work, the filters in Figures 1–4 and 6 are computed with data collected over the entire slug-test response, from early time until the dimensionless displacement in the well bore $H_{wb}(t)/H_{wb}(0)$ is less than 10^{-2}. Using early or late time data only, would lead to a different filter shape, and the effect of reducing the number of parameters by fixing the storage is evident by comparing Figures 1 and 6.

[52] While our analysis supports the observation that storage is poorly estimated by the slug test, the effect of storage on transmissivity estimates is more subtle. The most

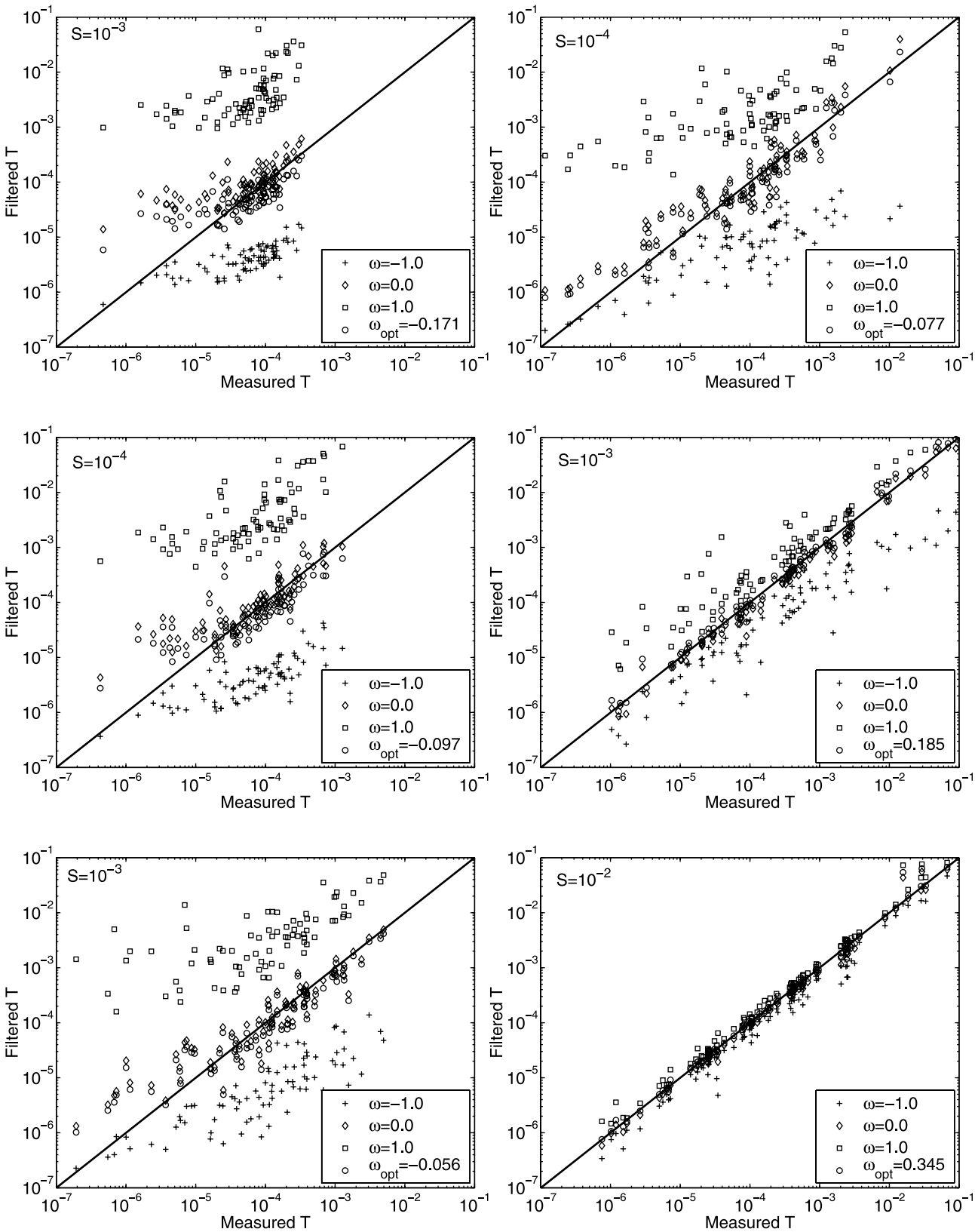

Figure 9. The same cross plots as found in Figure 7. To show the sensitivity of the power spatial filter to the power exponent ω, the plots here include transmissivities determined using the power spatial filter with the power exponent set to $\omega = -1, 0, +1$, in addition to the optimal values. Each point corresponds to one realization of a random field, and each figure (a–f) corresponds to a different ensemble. Ensemble statistics and the storage coefficient used for the simulations are provided in Table 1.

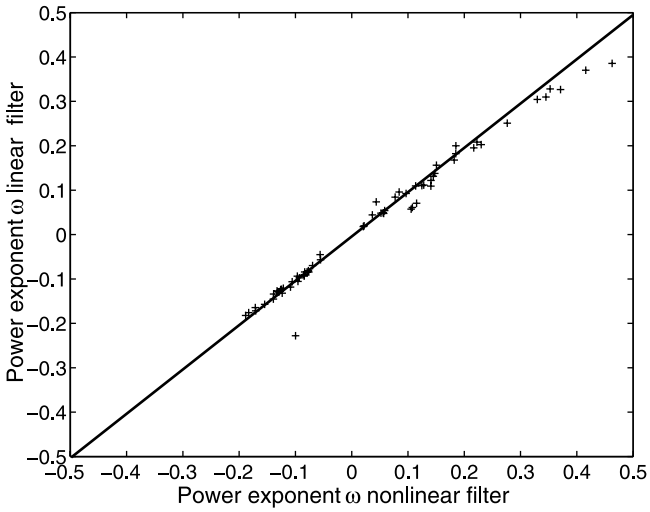

Figure 10. A cross plot showing the power exponent determined using the nonlinear power spatial filter expression versus the approximate spatial filter expression.

important effect is that on the *YY* filter functions in Figures 1 and 6. As storage decreases the support volumes of the *YY* filters increase. A second and smaller effect is through the *YS* filter function. Indeed, according to spatial-filter model (2.4), slug-test log transmissivity can be estimated from the smaller scale transmissivity by (for $\omega = 0$)

$$Y(x) = \int_V \mathcal{G}_{YY}(x - x')y(x')dx' + \int_V \mathcal{G}_{YS}(x - x')s(x')dx'. \quad (5.1)$$

In our investigation of heterogeneous aquifers, we are able to drop the second term since storage was spatially homogeneous and the *YS* filter in Figure 4b integrates to zero. If storage is not spatially homogeneous, then the smaller-scale storage will affect the value of the estimated log transmissivity through the *YS* term in (5.1) above, but the net effect still should be small, as the *YS* filter integrates to zero.

[53] The filtering approach we present here can be applied to estimation problems. The filter then provides a relationship between parameters measured on two different scales. Using the filtering relationship it is possible to develop estimation schemes where parameters measured on one scale are used to constrain parameter estimates on another scale [*Desbarats*, 1994].

6. Conclusions

[54] The measurement of transmissivity by the analysis of slug-test head-response data from a fully completed well in a confined aquifer can be represented as a weighted spatial power average of the log transmissivity proximal to the well. In our approach, the weighting is given by spatial filters that are functions of the aquifer storage. The power exponent of the power average depends upon the ratio of the integral scale of the log transmissivity field, λ to the r_a, the range or characteristic size of the filter functions. The power exponents that produce the best fit between the measured transmissivity and that predicted with the spatial filter, take values from $\omega = -0.19$ to $\omega = 0.345$, increasing as the ratio of heterogeneity size to slug-test averaging size λ/r_a increases. Even so, relatively good fits can be obtained for all fields with the power exponent of $\omega = 0$, which corresponds to geometric averaging. The fully nonlinear power averaging expression is also well approximated by an expression originally developed by *Desbarats* [1992], and which can be used in geostatistical estimation problems.

[55] Our results are somewhat encouraging for the usefulness of slug tests to estimate transmissivities, but indicate the dubious value of slug tests for estimating storage coefficients. The estimated transmissivity is unbiased, and is less sensitive to near-well heterogeneities in transmissivity because the estimated storage accounts for much of the effects of these near-well heterogeneities. The transmissivity estimate does not appear to be strongly influenced by storage coefficient properties. In contrast, the storage coefficient is strongly influenced by the transmissivity and the estimated storage is biased.

[56] The spatial filter functions provide insight into the volume measured by a slug test, but their application to field tests poses a dilemma: the filter function depends strongly upon the storage coefficient of the aquifer, yet the slug-test estimate of the storage coefficient is not likely to be correct. Thus the filter function may best be selected using independently estimated storage coefficients.

Appendix A

[57] In this appendix we describe the method we use to generate heterogeneous log transmissivity fields for a radial coordinate grid. We first generate a 2048 × 2048 log transmissivity field with square gridblocks and a prescribed correlation structure using a Fast Fourier Transformation technique [*Fenton*, 1990]. We then essentially map this field onto the radial grid using the following algorithm.

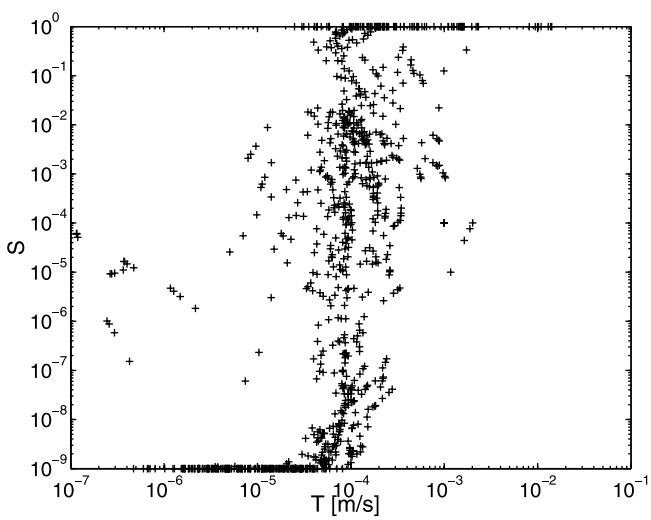

Figure 11. A cross plot showing estimated storage versus estimated transmissivity for a number of realizations where the true storage is 10^{-4}. Each point corresponds to a slug test analysis of data simulated in a different realization of the transmissivity field.

[58] We determine the radial and angular coordinates of the center of each the gridblock of the square grid from an origin at the center of the square grid. We then determine the gridblock of the radial grid that contains those coordinates and assign to that gridblock the value of log transmissivity from the square grid. Larger gridblocks of the radial grid may contain the center of many gridblocks from the square grid. In that case, the log transmissivity values from those square gridblocks are arithmetically averaged (or the transmissivity values are geometrically averaged). Where radial gridblocks are small near the well, some radial gridblocks are not assigned log transmissivity values after all the gridblocks from the square grid have been mapped. To those gridblocks we assign the log transmissivity value from the gridblock of the square grid that contains the coordinates of the centroid of the unassigned gridblock from the radial grid. As the square grid is typically somewhat smaller than the radial grid, some gridblocks of the radial grid at large radius also remain unassigned after each gridblock of the square grid is mapped. These unassigned distal gridblocks are assigned the average log transmissivity value of the square grid.

[59] The algorithm is admittedly a crude mapping. Alternatively, there are more elaborate approaches. One could define a statistical structure of a log transmissivity field at some fine scale. If radial gridblock log transmissivities were considered spatial averages of that fine-scale log transmissivity, then the local averaging theory presented by *Vanmarcke* [1983, chap. 6] could be used to determine the correlation between each pair of local averages of log transmissivities. The resulting covariance matrix could be used to generate realizations on the radial grid using the L-U decomposition method of *Alabert* [1987]. This general approach is not practical for the large 81×81 gridblock grid that we use here, and would not avoid the variable support scale problem that is encountered on the radial grid.

Appendix B

[60] In this appendix, we develop late time approximations for the Laplace domain solutions to the *Cooper et al.* [1967] homogeneous parameter model and the two-zone model of *Moench and Hsieh* [1985]. *Cooper et al.* [1967] provide the following Laplace domain solution to their model, given by equations (2.6)–(2.9),

$$\frac{\bar{h}_{wb}(p)}{H_{wb}(0)} = \frac{K_0(\beta)/p}{K_0(\beta) + \frac{2\alpha}{\beta}K_1(\beta)}, \tag{8.1}$$

where $\bar{h}_{wb}$ is the Laplace domain well bore head solution, p is the Laplace domain coordinate, K_0 and K_1 are modified Bessel functions of the second kind of zero and first order, respectively, $\alpha = S\left(\frac{r_w}{r_c}\right)^2$ and $\beta = r_w\sqrt{\frac{pS}{T}}$.

[61] The Laplace domain solution to the two-zone model of *Moench and Hsieh* [1985] is

$$\frac{\bar{h}_{wb}(p)}{H_{wb}(0)} = \frac{A[\Delta_1 K_0(B_1) - \Delta_2 l_0(B_1)]/p}{C_1\Delta_1 - C_2\Delta_2}, \tag{8.2}$$

where

$$C_1 = AK_0(B_1) + B_1K_1(B_1), \tag{8.3}$$

$$C_2 = Al_0(B_1) - B_1l_1(B_1),) \tag{8.4}$$

$$\Delta_1 = \frac{T_2}{T_1}l_0(B_1r_d')K_1(B_2r_d') + \sqrt{\frac{T_2}{T_1}}l_1(B_1r_d')K_0(B_2r_d'), \tag{8.5}$$

$$\Delta_2 = \frac{T_2}{T_1}K_0(B_1r_d')K_1(B_2r_d') + \sqrt{\frac{T_2}{T_1}}K_1(B_1r_d')K_0(B_2r_d'), \tag{8.6}$$

and where $A = \frac{pr_c^2}{2T_1}$, $B_1 = r_w\sqrt{\frac{pS}{T_1}}$ $B_2 = r_w\sqrt{\frac{pS}{T_2}}$, $r_d' = r'/r_w$, l_0, l_1 are the first and second order of the modified Bessel functions of the first kind.

[62] Late time approximations ($t \to \infty$ or $p \to 0$) to these solutions can be developed by using asymptotic approximations to the Bessel functions [e.g., *Sageev*, 1986], $K_0(x) \to -\ln(x)$, $K_1(x) \to 1/x$, $l_0(x) \to 1$ and $l_1(x) \to x/2$. The late time approximation to the *Cooper et al.* [1967] model is

$$\frac{\bar{h}_{wb}(p)}{H_{wb}(0)} = \frac{\ln\left(r_w\sqrt{\frac{pS}{T}}\right)}{p\left[\ln\left(r_w\sqrt{\frac{pS}{T}}\right)\right] - \frac{2T}{r_c^2}}. \tag{8.7}$$

[63] We produce a late time approximation to the two zone model of *Moench and Hsieh* [1985] substituting the asymptotic forms of the Bessel functions and by neglecting terms of order p in comparison to terms of order $\ln(p)$, terms of order p^2 in comparison to terms of order p and Last, r_w and r' are neglected in comparison to $r_c\sqrt{S}$. Neglecting r' in comparison to $r_c\sqrt{S}$ implies that the thickness of the inner zone must be small in comparison to the ratio of well bore storage to aquifer storage. The resulting late time approximation is

$$\frac{\bar{h}_{wb}(p)}{H_{wb}(0)} = \frac{\ln\left(r_w\sqrt{\frac{pS}{T_2}\left(\frac{r'}{r_w}\right)^{-2T_2/T_1-1}}\right)}{p\left\{\ln\left(r_w\sqrt{\frac{pS}{T_2}\left(\frac{r'}{r_w}\right)^{-2T_2/T_1-1}}\right) - \frac{2T_2}{r_c^2}\right\}}. \tag{8.8}$$

References

Alabert, F. G., The practice of fast conditional simulations through the LU decomposition of the covariance matrix, *Math. Geol.*, *19*(5), 369–386, 1987.

Barker, J. A, and J. H. Black, Slug tests in fissured aquifers, *Water Resour. Res.*, *19*(6), 1558–1564, 1983.

Beckie, R. D., A comparison of methods to determine measurement support volumes, *Water Resour. Res.*, *37*(4), 925–936, 2001.

Bouwer, H., The Bouwer Rice slug test - An update, *Ground Water*, *27*(3), 305–309, 1989.

Bouwer, H., and R. C. Rice, A slug tests for determining hydraulic conductivity of unconfined aquifers with completely or partially penetrating wells, *Water Resour. Res.*, *12*(3), 423–428, 1976.

Brown, D. L., T. N. Narasimhan, and Z. Demir, An evaluation of the Bouwer and Rice method of slug test analysis, *Water Resour. Res.*, *31*(5), 1239–1246, 1995.

Butler, J. J., Jr., and J. M. Healey, Relationship between pumping-test and slug-test parameters: Scale effect or artifact?, *Ground Water*, *36*(2), 305–313, 1998.

Butler, J. J., Jr., C. D. McElwee, and W. Liu, Improving the quality of parameter estimates obtained from slug tests, *Ground Water*, *34*(3), 480–490, 1996.

Cardwell, W. T., and R. L. Parsons, Average permeabilities of heterogeneous oil sands, *Trans. AIME*, *160*, 34–42, 1945.

Chirlin, G. R., A critique of the Hvorslev method for slug test analysis: The fully penetrating well, *Ground Water Monit. Rev.*, *9*(2), 130–138, 1989.

Cooper, H. H., J. D. Bredehoeft, and S. S. Papadopoulos, Response of a finite diameter well to an instantaneous charge of water, *Water Resour. Res.*, *3*(1), 263–269, 1967.

Dagan, G., A note on packer, slug, and recovery tests in unconfined aquifers, *Water Resour. Res.*, *14*(5), 929–934, 1978.

Dagan, G., Flow and Transport in Porous Formations, Springer-Verlag, New York, 1989.

Dax, A., A note on the analysis of slug tests, *J. Hydrol.*, *91*, 153–177, 1987.

Demir, Z., and T. N. Narasimhan, Improved interpretation of Hvorslev tests, *J. Hydraul. Eng.*, *120*(4), 1994.

Desbarats, A. J., Spatial averaging of transmissivity in heterogeneous fields with flow towards a well, *Water Resour. Res.*, *28*(3), 757–767, 1992.

Desbarats, A. J., Spatial averaging of hydraulic conductivity under radial flow conditions, *Math Geol.*, *26*(1), 1–21, 1994.

Faust, C. R., and J. W. Mercer, Evaluation of slug tests in wells containing a finite-thickness skin, *Water Resour. Res.*, *20*(4), 504–506, 1984.

Fenton, G. A., Simulation and analysis of random fields, Ph.D. thesis, Princeton Univ., Dep. of Civ. Eng., Princeton, N. J., 1990.

Guyonnet, D., S. Mishra, and J. McCord, Evaluating the volume of porous medium investigated during slug tests, *Ground Water*, *31*(4), 627–633, 1993.

Harvey, C. F., Interpreting parameter estimates obtained from slug tests in heterogeneous aquifers, M.Sc. thesis, Stanford Univ., Appl. Earth Sci. Dep., Stanford, Calif., 1992.

Hvorslev, M. J., Time-lag and soil permeability in ground-water observations, *Bull. 36*, pp. 1–50, Waterw. Exp. Stn., U.S. Army Corps of Eng., Vicksburg, Miss., 1951.

Hyder, Z., and J. J. Butler Jr., Slug tests in unconfined formations: An assessment of the Bower and Rice technique, *Ground Water*, *33*(1), 16–22, 1995.

Hyder, Z., J. J. Butler Jr., C. D. McElwee, and W. Z. Liu, Slug tests in partially penetrating wells, *Water Resour. Res.*, *30*(11), 2945–2957, 1994.

Jaeger, J. C., Radial heat flow in circular cylinders with a general boundary condition, *R. Soc. N. S. W. J. and Proc.*, *74*, 342–352, 1940.

Jaeger, J. C., Conduction of heat in an infinite region bounded internally by circular cylinder of a perfect conductor, *Aust. J. Phys.*, *9*, 167–179, 1955.

Karasaki, K., J. C. S. Long, and P. A. Witherspoon, Analytical models of slug tests, *Water Resour. Res.*, *24*(1), 115–126, 1988.

McElwee, C. D., G. C. Bohling, and J. J. Butler Jr., Sensitivity analysis of slug tests, part 1, The slugged well, *J. Hydrol.*, *164*, 53–67, 1995a.

McElwee, C. D., J. J. Butler Jr., G. C. Bohling, and W. Liu, Sensitivity analysis of slug tests, part 2, Observation wells, *J. Hydrol.*, *164*, 69–87, 1995b.

Moench, A. F., and P. A. Hsieh, Analysis of slug test data in a well with finite-thickness skin, in *Memoirs of the 17th International Congress on the Hydrogeology of Rocks of Low Permeability*, pp. 17–29, Int. Assoc. of Hydrol., Tucson, Ariz., 1985.

Narasimhan, T. N., Geometry imbedded Darcy's law and transient subsurface flow, *Water Resour. Res.*, *21*(8), 1285–1292, 1985.

Novakowski, K., Analysis of pulse interference tests, *Water Resour. Res.*, *25*(11), 2377–2387, 1989.

Pandit, N. S., and R. F. Miner, Interpretation of slug test data, *Ground Water*, *24*(6), 743–749, 1986.

Peres, A. M., M. Onur, and A. C. Reynolds, A new analysis procedure for determining aquifer properties from slug test data, *Water Resour. Res.*, *25*(7), 1591–1602, 1989.

Ramey, H. J., Jr., R. G. Agarwal, and I. Martin, Analysis of "Slug test" or DST flow period data, *Can. J. Pet. Technol.*, 37–47, 1975.

Sageev, A., Slug test analysis, *Water Resour. Res.*, *22*(8), 1323–1333, 1986.

Townley, L., and J. L. Wilson, Computationally efficient algorithms for parameter estimation and uncertainty propagation in numerical models of groundwater flow, *Water Resour. Res.*, *21*(12), 1851–1860, 1985.

Vanmarcke, E., *Random Fields: Analysis and Synthesis*, MIT Press, Cambridge, Mass., 1983.

Wang, B., The spatial filtering from core-scale conductivity to the conductivity measured by a slug test, M.A.Sc. thesis, Univ. of British Columbia, Dep. of Geol. Sci., Vancouver, B. C., pp. 218, 1995.

Widdowson, M. A., F. J. Molz, and J. G. Melville, An analysis technique for multilevel and partially penetrating slug test data, *Ground Water*, *28*(6), 937–945, 1990.

Yang, Y. J., and T. M. Gates, Wellbore skin effect in slug-test data analysis for low-permeability geologic materials, *Ground Water*, *35*(6), 931–937, 1997.

Zlotnik, V., Interpretation of slug and packer tests in anisotropic aquifers, *Ground Water*, *32*(5), 761–767, 1994.

R. Beckie, Department of Earth and Ocean Sciences, University of British Columbia, 6339 Stores Road, Vancouver, British Columbia, Canada V6T 1Z4. (rbeckie@eos.ubc.ca)

C. F. Harvey, Ralph M. Parsons Laboratory, Department of Civil and Environmental Engineering, Massachusetts Institute of Technology, 48-321, 15 Vasser St., Cambridge, MA 02139, USA. (charvey@mit.edu)